

## **Supplementary Material**

for

Cobalt(II) “Scorpionate” Complexes as Models for Co-substituted Zinc  
Enzymes: Electronic Structure Investigation by High-Frequency and -Field  
Electron Paramagnetic Resonance Spectroscopy

J. Krzystek, Dale C. Swenson, S. A. Zvyagin, Dmitry Smirnov, Andrew Ozarowski, and  
Joshua Telser\*

## Discussion of Crystallographically Determined Structures of $\text{Tp}^{\text{R,R'}}\text{CoL}$ Complexes.

The crystal and molecular structures of numerous scorpionate complexes of Co(II) have been reported, with coordination numbers of 4, 5, and 6.<sup>1</sup> Of relevance here are four-coordinate complexes of general formula  $\text{Tp}^{\text{R,R'}}\text{CoL}$ , where L is  $\text{Cl}^-$ ,  $\text{NCS}^-$ ,  $\text{NCO}^-$ , and  $\text{N}_3^-$ . One could make detailed comparisons among these complexes with regards to the scorpionate ligand metrics, however, there appears to be nothing remarkable about these, and our chief interest is the inner coordination sphere of the Co(II) ion. Thus, the relevant factors are the metal-ligand bond lengths and angles, which are summarized in Table 1 (main text). The crystallographic information is given here in Table S1 and more extensive geometric parameters are given in Table S2. These geometric parameters will be treated as a group for all  $\text{Tp}^{\text{R,R'}}\text{CoL}$  complexes.

We begin by discussing the chloro complexes, as this is the simplest L. A search of the Cambridge Structural Database at the onset of this study (November 2005 release) revealed four complexes of type  $\text{Tp}^{\text{R,R'}}\text{CoCl}$ , along with analogues that are pentacoordinate due to an additional unidentate ligand. These four are the following, identified by pyrazole ring substituents: (3-*t*-Bu),<sup>2</sup> (3-*i*-Pr,4-*t*-Bu),<sup>3</sup> (3-Ph,5-Me),<sup>4</sup> and (3-*i*-Pr,4-Br).<sup>5</sup> During the course of this study, the structure of the complex with (3-*t*-Bu,5-Me) was reported;<sup>6</sup> however, we found different crystallographic parameters for this same complex and thus report our results as well. To these we add a previously unreported structure, (3-*t*-Bu,5-Tn).

Thiocyanato-coordinated scorpionate complexes of Co(II) are also relatively numerous; besides the present structures, (3-*t*-Bu,5-Me) and (3-*t*-Bu,5-Tn), these comprise the following: (3-*t*-Bu),<sup>7</sup> (3-*i*-Pr,4-Br),<sup>8</sup> (3-*i*-Pr,4-*t*-Bu),<sup>3</sup> and several compounds

with unsymmetrically substituted scorpionate ligands: [(3-*t*-Bu)<sub>2</sub>(3-Ph)],<sup>9</sup> [(3,5-*t*-Bu)(3-Ph)<sub>2</sub>],<sup>10</sup> and [(7-*t*-butylindazol-2-yl)<sub>2</sub>(7-*t*-butylindazol-1-yl)], in which a symmetrically substituted ligand rearranged to give an unsymmetrical complex.<sup>11</sup> The relevant metrical information is given in Table 1.

In contrast to the cases for L = Cl<sup>-</sup> and NCS<sup>-</sup>, for L = NCO<sup>-</sup>, there is also only one previously reported structure of a Co(II) scorpionate complex, regardless of coordination number: (3-Np) (Np = neopentyl).<sup>12</sup> The present study adds significantly to this number by providing data on two more complexes. In addition to the metal-ligand bond lengths and angles, the tilt of the cyanato ligand is also of interest and is given in Table 1.

For L = N<sub>3</sub><sup>-</sup>, there is also only one previously reported structure of a Co(II) scorpionate complex, regardless of coordination number: that with R = 3-*i*-Pr, R' = 4-*t*-Bu.<sup>3</sup> Moreover, to our knowledge, this is the only previous example of a structurally characterized four-coordinate azido complex of Co(II). Indeed, structurally characterized mononuclear complexes of Co(II) with unidentate azido ligands of whatever geometry are relatively rare: the CSD (November 2007 release) yields only 20 such structures; the most relevant are complexes of general form [Co(L)(N<sub>3</sub>)<sub>1-2</sub>]<sup>0,+</sup>, where L = a multidentate or macrocyclic N-donor ligand; there are structures of a slightly larger number of di- and polynuclear Co(II) azido complexes and roughly 100 azido complexes of Co(III). The present study adds two more Co(II)-azido complexes to the structural database. In addition to the metal-ligand bond lengths and angles, the tilt of the azido ligand is also of interest and is given in Table 1. This angle is smaller than that for the cyanato and thiocyanato complexes: ~135° – 150° versus ~160° – 180° for NC(O,S).

Inspection of Table 1 reveals no peculiarities about the structures of  $\text{Tp}^{\text{R,R'}}\text{CoL}$  complexes, despite the extensive variation in pyrazole substituent groups. The Co-N(pyrazole-N2) bond distances fall within a rather narrow range, with the mean and standard deviation of all of the distances listed having the values 2.027 Å and 0.009 Å, respectively. Indeed, the variation in metrical parameters between the two crystallographically distinct molecules of  $\text{Tp}^{i\text{-Pr},t\text{-Bu}}\text{CoN}_3$ <sup>3</sup> is nearly as much as among any different complexes. Similarly, the variation between the two structures reported (this work and Ferrence and Beitelman<sup>6</sup>) for  $\text{Tp}^{t\text{-Bu,Me}}\text{CoCl}$  is comparable to that between any two different chloro complexes.

The ten complexes studied herein by HFEP, which have been structurally characterized, here or by others:<sup>2, 7</sup>  $\text{Tp}^{t\text{-Bu,H}}\text{CoL}$ ,  $\text{L} = \text{Cl}^-$ ,  $\text{NCS}^-$ ,  $\text{NCO}^-$ ,  $\text{N}_3^-$ ;  $\text{Tp}^{t\text{-Bu,Me}}\text{CoL}$ ,  $\text{L} = \text{Cl}^-$ ,  $\text{NCS}^-$ ,  $\text{NCO}^-$ ,  $\text{N}_3^-$ ; and  $\text{Tp}^{t\text{-Bu,Tn}}\text{CoL}$ ,  $\text{L} = \text{Cl}^-$ ,  $\text{NCS}^-$ , exhibit Co-N bond distances that are towards the upper end of this range for  $\text{L} = \text{Cl}^-$ ,  $\text{NCO}^-$ ,  $\text{N}_3^-$  (mean of these six: 2.034 Å), and towards the lower end for  $\text{L} = \text{NCS}^-$  (mean of these three: 2.018 Å), but none is remarkable. Concerning the Co-L bond distances, there is a sufficient number of complexes overall for  $\text{L} = \text{Cl}^-$  (8 complexes/structures) and  $\text{NCS}^-$  (9 complexes) to make a comparison for specific L. The mean and standard deviation of the Co-Cl distances are 2.211 Å and 0.006 Å, respectively, with the two complexes studied here towards the upper end of this admittedly tight grouping. The mean and standard deviation of the Co-N(CS) distances are 1.913 Å and 0.007 Å, respectively, with the three complexes studied here in the middle of the range. The mean and standard deviation of all of the Co-N(CO,CS,N<sub>2</sub>) distances (15 complexes) are 1.912 Å and 0.008 Å, respectively, with the cyanato and azido complexes studied here well within this range.

The L tilt, Co-N-(CO,CS,N<sub>2</sub>) angle, has a mean and standard deviation for Co-N-C(S) of 170.00° and 3.46°, respectively, with the three complexes studied here roughly within  $\pm\sigma$ . As mentioned above, there is only one other structurally characterized example for each of the cyanato and azido complexes. It is somewhat counterintuitive that the tilt angles for the previously reported cyanato and azido complexes, which generally have bulkier R,R' groups, are each very close to those for Tp<sup>t-Bu,H</sup>Co(NCS, N<sub>3</sub>) (within 4°; indeed, the tilt angle for Tp<sup>t-Bu,H</sup>CoN<sub>3</sub> is closer to that for one of the crystallographically distinct molecules in Tp<sup>i-Pr,4-t-Bu</sup>CoN<sub>3</sub> than the two are to each other) while the Tp<sup>t-Bu,H</sup>Co(NCS, N<sub>3</sub>) complexes are the outliers (differing by ~10 – 15° from the angles in the other two complexes).

The other important bond angles about the Co(II) ion likewise contain few surprises. With the exception of the highly unsymmetrical indazole complex reported by Rheingold et al.,<sup>11</sup> which is not a pyrazole in any case, essentially all of the L-Co-N(pyrazole-N2) bond angles fall within the range 114 – 124°, with a mean value of 121.53° and standard deviation of 0.79°. This angle defines the  $\theta$  coordinate in the AOM analysis described in the main text. The complexes studied by HFEPR exhibit L-Co-N bond angles in the range 114 – 124°, but the spread for a given L is quite small: the Cl-Co-N(pz) bond angles are 118 – 122° for the three chloro complexes studied by HFEPR. The final angle of relevance is the N(pyrazole-N1)<sub>i</sub>-B-Co-N(pyrazole-N2)<sub>j</sub> torsional angle, where *i, j* are pyrazole ring identifiers, *i* = 1 – 3, *j* = 1 – 3, *j* ≠ *i*. This angle defines the  $\phi$  coordinate in the AOM analysis described below. Due to slight twisting of the pyrazole rings, a given pair of angles, N(pyrazole-N1)<sub>i</sub>-B-Co-N(pyrazole-N2)<sub>j</sub> and N(pyrazole-N1)<sub>j</sub>-B-Co-N(pyrazole-N2)<sub>i</sub>, are typically unequal (except for Tp<sup>t-Bu,Me</sup>CoCl,

which has three-fold crystallographic symmetry). The mean of these angles is by definition exactly  $120^\circ$  since we are projecting the complex onto a circle and dividing it into three angles, thus the deviation from this ideal value is what is only relevant and it is very small:  $\sigma = 1.83^\circ$ , using all complexes listed with each of their individual angles. Of the structurally characterized complexes studied here by HFEPR, all show deviations in this angle by at most  $\sim 2^\circ$ , except for  $\text{Tp}^{t\text{-Bu,Tn}}\text{Co}(\text{NCS})$ , where the angles deviate by as much as  $6^\circ$ .

To summarize the above discussion, the structurally characterized complexes studied here by HFEPR are entirely typical of  $\text{Tp}^{\text{R,R'}}\text{CoL}$  complexes in terms of both the Tp and L coordination. They furthermore closely approximate  $C_{3v}$  point group symmetry. Indeed,  $\text{Tp}^{t\text{-Bu,Me}}\text{CoCl}$ , as determined here, is especially significant as it exhibits crystallographic three-fold symmetry (space group  $R3m$ ), alone among the structurally characterized  $\text{Tp}^{\text{R,R'}}\text{CoL}$  complexes (the previously reported structure for this complex exhibits only a mirror plane).

**Table S1.** Crystal, data collection, and refinement parameters for  $\text{Tp}^{t\text{-Bu},\text{R}'}\text{CoL}$  complexes.

Complex	$\text{Tp}^{t\text{-Bu},\text{Tn}}\text{CoCl}$	$\text{Tp}^{t\text{-Bu},\text{Tn}}\text{CoNCS}$	$\text{Tp}^{t\text{-Bu},\text{H}}\text{CoNCO}$	$\text{Tp}^{t\text{-Bu},\text{H}}\text{CoN}_3$	$\text{Tp}^{t\text{-Bu},\text{Me}}\text{CoCl}$
Crystal data					
Chemical formula	$\text{C}_{33}\text{H}_{40}\text{BClCoN}_6\text{S}_3\cdot\text{CH}_2\text{Cl}_2$	$\text{C}_{34}\text{H}_{40}\text{BCoN}_7\text{S}_4$	$\text{C}_{22}\text{H}_{34}\text{BCoN}_7\text{O}$	$\text{C}_{21}\text{H}_{34}\text{BCoN}_9$	$\text{C}_{24}\text{H}_{40}\text{BClCoN}_6$
$M_r$	807.01	744.71	482.30	482.31	517.81
Cell setting, space group	Monoclinic, $C2/c$	Monoclinic, $P2(1)/n$	Monoclinic, $P2(1)/n$	Monoclinic, $P2(1)/n$	Trigonal, $R3m$
Temperature (K)	190 (2)	190 (2)	90 (2)	190 (2)	190 (2)
$a, b, c$ (Å)	37.859 (4), 9.7245 (10), 23.612 (2)	9.8456 (10), 27.114 (3), 14.1270 (14)	10.0557 (10), 16.0979 (16), 15.8729 (16)	10.1577 (11), 15.8814 (17), 15.8027 (17)	15.9843 (17), 15.9843 (17), 9.4269 (10)
$\alpha, \beta, \gamma$ (°)	90.00, 111.508 (5), 90.00	90.00, 92.325 (5), 90.00	90.00, 91.405 (5), 90.00	90.00, 91.186 (5), 90.00	90.00, 90.00, 120.00
$V$ (Å <sup>3</sup> )	8087.7 (14)	3768.1 (7)	2568.7 (4)	2548.7 (5)	2085.9 (4)
$Z$	8	4	4	4	3
$D_x$ (Mg m <sup>-3</sup> )	1.326	1.313	1.247	1.257	1.237
Radiation type	Mo $K\alpha$	Mo $K\alpha$	Mo $K\alpha$	Mo $K\alpha$	Mo $K\alpha$
$\mu$ (mm <sup>-1</sup> )	0.81	0.71	0.70	0.70	0.74
Crystal form, color	Needle, blue	Plate, blue	Plate, blue	Prism, blue	Needle, blue
Crystal size (mm)	0.38 × 0.04 × 0.04	0.19 × 0.13 × 0.06	0.22 × 0.20 × 0.02	0.25 × 0.21 × 0.14	0.30 × 0.06 × 0.05
Data collection					
Diffractometer	Nonius KappaCCD	Nonius KappaCCD	Nonius KappaCCD	Nonius KappaCCD	Nonius KappaCCD
Data collection method	CCD phi and $\omega$ scans	CCD phi and $\omega$ scans	CCD phi and $\omega$ scans	CCD phi and $\omega$ scans	CCD phi and $\omega$ scans
Absorption correction	Multi-scan (based on symmetry-related measurements)	Multi-scan (based on symmetry-related measurements)	Multi-scan (based on symmetry-related measurements)	Multi-scan (based on symmetry-related measurements)	Multi-scan (based on symmetry-related measurements)
$T_{\min}$	0.749	0.877	0.862	0.845	0.809
$T_{\max}$	0.972	0.959	0.986	0.908	0.964
No. of measured, independent and observed reflections	68370, 7128, 4920	54745, 8614, 6123	41469, 5874, 3610	53457, 5840, 4806	9505, 1175, 1148

Criterion for observed reflections	$I > 2\sigma(I)$	$I > 2\sigma(I)$	$I > 2\sigma(I)$	$I > 2\sigma(I)$	$I > 2\sigma(I)$
$R_{\text{int}}$	0.070	0.052	0.099	0.033	0.035
$\theta_{\text{max}}$ (°)	25.0	27.5	27.5	27.5	27.5
Refinement					
Refinement on	$F^2$	$F^2$	$F^2$	$F^2$	$F^2$
$R[F^2 > 2\sigma(F^2)]$ , $wR(F^2)$ , $S$	0.059, 0.162, 1.06	0.039, 0.093, 1.05	0.048, 0.099, 1.01	0.037, 0.096, 1.11	0.023, 0.056, 1.09
No. of reflections	7128 reflections	8614 reflections	5874 reflections	5840 reflections	1175 reflections
No. of parameters	448	463	289	299	70
H-atom treatment	Constrained to parent site	Constrained to parent site	Constrained to parent site	Constrained to parent site	Mixture of independent and constrained refinement
Weighting scheme	Calculated $w = 1/[\sigma^2(F_o^2) + (0.0783P)^2 + 18.7685P]$ where $P = (F_o^2 + 2F_c^2)/3$	Calculated $w = 1/[\sigma^2(F_o^2) + (0.0366P)^2 + 0.9706P]$ where $P = (F_o^2 + 2F_c^2)/3$	Calculated $w = 1/[\sigma^2(F_o^2) + (0.0373P)^2 + 0.2747P]$ where $P = (F_o^2 + 2F_c^2)/3$	Calculated $w = 1/[\sigma^2(F_o^2) + (0.0351P)^2 + 1.5074P]$ where $P = (F_o^2 + 2F_c^2)/3$	Calculated $w = 1/[\sigma^2(F_o^2) + (0.0297P)^2 + 0.7201P]$ where $P = (F_o^2 + 2F_c^2)/3$
$(\Delta/\sigma)_{\text{max}}$	0.009	0.002	0.002	0.001	0.001
$\Delta\rho_{\text{max}}$ , $\Delta\rho_{\text{min}}$ (e $\text{\AA}^{-3}$ )	0.83, -0.91	0.52, -0.43	0.28, -0.28	0.35, -0.32	0.18, -0.22
Extinction method	None	None	None	SHELXL	None
Extinction coefficient				0.0050 (7)	
Absolute structure					Flack, H. D. (1983), <i>Acta Cryst.</i> A39, 876-881
Flack parameter					0.442 (15)
Rogers parameter					

Complex	Tp <sup>t-Bu,Me</sup> CoNCS	Tp <sup>t-Bu,Me</sup> CoNCO	Tp <sup>t-Bu,Me</sup> CoN <sub>3</sub>
Crystal data			
Chemical formula	C <sub>25</sub> H <sub>40</sub> BCoN <sub>7</sub> S	C <sub>25</sub> H <sub>40</sub> BCoN <sub>7</sub> O	(C <sub>24</sub> H <sub>40</sub> BCoN <sub>9</sub> ) 0.5(C <sub>7</sub> H <sub>8</sub> )
<i>M<sub>r</sub></i>	540.44	524.38	570.46
Cell setting, space group	Monoclinic, <i>P2<sub>1</sub>/n</i>	Monoclinic, <i>P2<sub>1</sub>/n</i>	Monoclinic, <i>P2<sub>1</sub>/n</i>
Temperature (K)	190 (2)	190 (2)	190 (2)
<i>a</i> , <i>b</i> , <i>c</i> (Å)	9.6545 (11), 17.4408 (18), 17.9183 (18)	10.4823 (11), 17.0139 (18), 16.0436 (17)	10.5385 (12), 19.126 (2), 15.7062 (17)
$\alpha$ , $\beta$ , $\gamma$ (°)	90.00, 98.059 (5), 90.00	90.00, 91.101 (5), 90.00	90.00, 90.437 (5), 90.00
<i>V</i> (Å <sup>3</sup> )	2987.3 (5)	2860.8 (5)	3165.6 (6)
<i>Z</i>	4	4	4
<i>D<sub>x</sub></i> (Mg m <sup>-3</sup> )	1.202	1.218	1.197
Radiation type	Mo <i>K</i> α	Mo <i>K</i> α	Mo <i>K</i> α
$\mu$ (mm <sup>-1</sup> )	0.67	0.63	0.57
Crystal form, colour	Plate, blue	Plate, blue	Plate, blue
Crystal size (mm)	0.33 × 0.27 × 0.03	0.38 × 0.22 × 0.05	0.33 × 0.19 × 0.01
Data collection			
Diffractometer	Nonius KappaCCD	Nonius KappaCCD	Nonius KappaCCD
Data collection method	CCD phi and $\omega$ scans	CCD phi and $\omega$ scans	CCD phi and $\omega$ scans
Absorption correction	Multi-scan (based on symmetry-related measurements)	Multi-scan (based on symmetry-related measurements)	Multi-scan (based on symmetry-related measurements)
	0.809	0.796	0.833

*T<sub>min</sub>*

	0.984	0.966	0.994
$T_{\max}$			
No. of measured, independent and observed reflections	54226, 6838, 4399	59524, 6790, 4684	48065, 5569, 4229
Criterion for observed reflections	$I > 2\sigma(I)$	$I > 2\sigma(I)$	$I > 2\sigma(I)$
$R_{\text{int}}$	0.079	0.051	0.054
$\theta_{\max}$ (°)	27.5	27.9	25.0
Refinement			
Refinement on	$F^2$	$F^2$	$F^2$
$R[F^2 > 2\sigma(F^2)]$ , $wR(F^2)$ , $S$	0.043, 0.101, 1.03	0.044, 0.111, 1.03	0.046, 0.117, 1.03
No. of reflections	6838 reflections	6790 reflections	5569 reflections
No. of parameters	328	341	371
H-atom treatment	Constrained to parent site	Constrained to parent site	Constrained to parent site
Weighting scheme	Calculated $w = 1/[\sigma^2(F_o^2) + (0.0416P)^2 + 0.668P]$ where $P = (F_o^2 + 2F_c^2)/3$	Calculated $w = 1/[\sigma^2(F_o^2) + (0.0467P)^2 + 1.1178P]$ where $P = (F_o^2 + 2F_c^2)/3$	Calculated $w = 1/[\sigma^2(F_o^2) + (0.0473P)^2 + 3.4331P]$ where $P = (F_o^2 + 2F_c^2)/3$
$(\Delta/\sigma)_{\max}$	0.001	<0.0001	0.009
$\Delta\rho_{\max}, \Delta\rho_{\min}$ (e Å <sup>-3</sup> )	0.30, -0.33	0.26, -0.56	0.58, -0.42
Extinction method	None	None	None
Extinction coefficient			
Absolute structure			
Flack parameter			
Rogers parameter			

**Table S2.** Geometric parameters for  $\text{Tp}^{t\text{-Bu,R}'}\text{CoL}$  complexes investigated here as determined by x-ray crystallography.

Geometric parameter (Å, °)	$\text{Tp}^{t\text{-Bu,H}}\text{Co}$ NCO	$\text{Tp}^{t\text{-Bu,H}}\text{Co}$ N <sub>3</sub>	$\text{Tp}^{t\text{-Bu,Me}}\text{Co}$ Cl	$\text{Tp}^{t\text{-Bu,Me}}\text{Co}$ NCS	$\text{Tp}^{t\text{-Bu,Me}}\text{Co}$ NCO	$\text{Tp}^{t\text{-Bu,Me}}\text{Co}$ N <sub>3</sub>	$\text{Tp}^{t\text{-Bu,Tn}}\text{Co}$ Cl	$\text{Tp}^{t\text{-Bu,Tn}}\text{Co}$ NCS
Co1-N1	2.031(2)	2.035(2)	2.029(2)	2.003(2)	2.031(2)	2.030(2)	2.040(3)	2.019(2)
Co1-N3	2.037(2)	2.032(2)		2.023(2)	2.026(2)	2.030(2)	2.042(3)	2.018(2)
Co1-N5	2.024(2)	2.035(2)		2.018(2)	2.011(2)	2.039(2)	2.038(3)	2.022(2)
Co1-Cl(N)	1.906(2)	1.919(2)	2.2202(10)	1.915(2)	1.916(2)	1.917(3)	2.2181(12)	1.916(2)
B1-N2	1.543(3)	1.542(3)	1.550(2)	1.558(3)	1.547(3)	1.548(4)	1.548(6)	1.558(3)
B1-N4	1.546(3)	1.545(3)		1.550(3)	1.547(3)	1.543(4)	1.540(5)	1.548(3)
B1-N6	1.544(3)	1.547(3)		1.549(3)	1.546(3)	1.546(4)	1.551(5)	1.554(3)
N1-N2	1.377(3)	1.377(2)	1.378(2)	1.386(2)	1.381(2)	1.383(3)	1.386(4)	1.377(2)
N3-N4	1.382(3)	1.377(2)		1.386(2)	1.378(2)	1.385(3)	1.383(4)	1.376(2)
N5-N6	1.378(3)	1.379(2)		1.387(2)	1.385(3)	1.377(3)	1.382(4)	1.379(2)
N-C(N)	1.166(3)	1.178(3)		1.169(3)	1.129(3)	1.091(12)	-	1.165(3)
C(N)-S(O)(N)	1.194(3)	1.156(3)		1.608(2)	1.208(3)	1.184(6)	-	1.599(2)
N1-Co1-N3	94.60(8)	95.16(6)	95.18(7)	95.75(7)	97.36(7)	94.48(9)	93.96(13)	95.73(6)
N1-Co1-N5	94.62(8)	95.87(6)		94.63(7)	96.09(7)	96.60(9)	95.81(13)	95.61(6)
N3-Co1-N5	96.13(8)	94.11(6)		97.67(7)	93.52(7)	94.21(9)	96.61(13)	94.26(6)
N1-Co1-Cl(N)	122.77(8)	117.91(8)	121.51(5)	121.57(8)	118.57(8)	119.5(7)	123.62(10)	122.51(7)
N3-Co1-Cl(N)	119.75(9)	122.47(8)		120.81(8)	122.73(8)	122.4(5)	121.41(10)	119.81(7)
N5-Co1-Cl(N)	122.14(9)	124.39(8)		120.26(8)	122.19(9)	122.8(4)	118.90(10)	122.11(7)
N2-B1-N4	108.4(2)	109.68(16)	109.16(16)	109.5(2)	109.9(2)	110.0(2)	109.3(3)	110.3(2)
N2-B1-N6	109.9(2)	109.21(16)		108.9(2)	110.0(2)	109.6(2)	110.0(3)	107.5(2)
N4-B1-N6	109.4(2)	108.13(15)		108.9(2)	109.0(2)	109.3(2)	110.1(3)	109.5(2)
Co1-N1-N2	110.23(14)	109.31(11)	110.15(13)	109.56(12)	109.64(12)	109.82(16)	109.4(2)	110.07(11)
Co1-N3-N4	110.08(14)	110.16(11)		109.26(13)	109.97(12)	110.10(15)	108.9(2)	110.03(11)
Co1-N5-N6	109.59(14)	110.16(11)		109.50(12)	109.66(13)	110.44(16)	110.3(2)	110.69(11)
Co1-N-C(N)	158.3(2)	140.0(2)		175.7(2)	176.1(2)	148.6(14)	-	166.8(2)
N-C(N)-S(O)	179.7(4)	176.8(2)		179.5(3)	178.9(3)	177.6(100)	-	178.9(2)
B1-N2-N1	121.0(2)	122.37(15)	121.1(2)	120.88(17)	120.61(16)	121.0(2)	120.9(3)	120.33(15)
B1-N4-N3	120.9(2)	121.36(15)		121.10(17)	120.24(16)	120.7(2)	121.7(3)	120.84(15)
B1-N6-N5	121.9(2)	121.23(15)		120.29(16)	120.87(17)	120.4(2)	120.0(3)	120.07(14)

**Table S3.**

Electronic absorption data for  $\text{Tp}^{\text{R,R'}}\text{CoL}$  ( $\text{R} = t\text{-Bu}$ ,  $\text{R}' = \text{H}$ ,  $\text{Me}$ ,  $\text{Tn}$ ;  $\text{L} = \text{NCS}^-$ ,  $\text{NCO}^-$ ,  $\text{N}_3^-$ ,  $\text{Cl}^-$ ) complexes in  $\text{CCl}_4$  solution at room temperature. Uncertainty in wavelengths is  $\pm 1$  nm (in wavenumbers,  $\pm 30$   $\text{cm}^{-1}$ ).

L =	$\text{NCS}^-$	$\text{NCO}^-$	$\text{N}_3^-$	$\text{Cl}^-$
	( $\epsilon$ , ( $\text{mol/L}$ ) $^{-1}\text{cm}^{-1}$ )	( $\epsilon$ , ( $\text{mol/L}$ ) $^{-1}\text{cm}^{-1}$ )	( $\epsilon$ , ( $\text{mol/L}$ ) $^{-1}\text{cm}^{-1}$ )	( $\epsilon$ , ( $\text{mol/L}$ ) $^{-1}\text{cm}^{-1}$ )
$\text{Tp}^- =$ $\text{Tp}^{t\text{-Bu,H}}$	1520 nm, 6580 $\text{cm}^{-1}$ (140) 938 nm, 10660 $\text{cm}^{-1}$ (260) 660 nm, 15150 $\text{cm}^{-1}$ (sh) (850) 643 nm, 15550 $\text{cm}^{-1}$ (1640) 629 nm, 15900 $\text{cm}^{-1}$ (sh) (1480) 595 nm, 16810 $\text{cm}^{-1}$ (sh) (880) 540 nm, 18520 $\text{cm}^{-1}$ (sh) (160)	1550 nm, 6450 $\text{cm}^{-1}$ (40) 908 nm, 11010 $\text{cm}^{-1}$ (30) 666 nm, 15020 $\text{cm}^{-1}$ (350) 646 nm, 15480 $\text{cm}^{-1}$ (300) 615 nm, 16260 $\text{cm}^{-1}$ (240) 584 nm, 17120 $\text{cm}^{-1}$ (160) 540 nm, 18520 $\text{cm}^{-1}$ (sh) (30)	1540 nm, 6490 $\text{cm}^{-1}$ (300) 924 nm, 10820 $\text{cm}^{-1}$ (290) 676 nm, 14790 $\text{cm}^{-1}$ (3520) 666 nm, 15020 $\text{cm}^{-1}$ (sh) (3280) 639 nm, 15650 $\text{cm}^{-1}$ (sh) (2280) 597 nm, 16750 $\text{cm}^{-1}$ (sh) (1130) 550 nm, 18180 $\text{cm}^{-1}$ (sh) (360)	1650 nm, 6060 $\text{cm}^{-1}$ (45) 956 nm, 10460 $\text{cm}^{-1}$ (40) --- 663 nm, 15080 $\text{cm}^{-1}$ (360) 633 nm, 15800 $\text{cm}^{-1}$ (410) 601 nm, 16640 $\text{cm}^{-1}$ (sh) (250) 547 nm, 18280 $\text{cm}^{-1}$ (sh) (30)
$\text{Tp}^{t\text{-Bu,Me}}$	1505 nm, 6640 $\text{cm}^{-1}$ (130) 935 nm, 10690 $\text{cm}^{-1}$ (280)  658 nm, 14800 (sh) $\text{cm}^{-1}$ (930) 638 nm, 15680 $\text{cm}^{-1}$ (1260) 596 nm, 16760 $\text{cm}^{-1}$ (sh) (750) --- 530 nm, 18760 $\text{cm}^{-1}$ (sh) (60)	1545 nm, 6460 $\text{cm}^{-1}$ (70) 925 nm, 10820 $\text{cm}^{-1}$ (70)  662 nm, 15510 $\text{cm}^{-1}$ (500) 642 nm, 15590 $\text{cm}^{-1}$ (500) 618 nm, 16200 $\text{cm}^{-1}$ (450) 590 nm, 17050 $\text{cm}^{-1}$ (sh) (290) 525 nm, 19150 $\text{cm}^{-1}$ (sh) (40)	1535 nm, 6500 $\text{cm}^{-1}$ (230) 918 nm, 10890 $\text{cm}^{-1}$ (280)  667 nm, 15000 $\text{cm}^{-1}$ (2300) 642 nm, 15600 $\text{cm}^{-1}$ (sh) (1900) 600 nm, 16650 $\text{cm}^{-1}$ (sh) (940) --- 542 nm, 18300 $\text{cm}^{-1}$ (sh) (170)	1640 nm, 6080 $\text{cm}^{-1}$ (110) 947 nm, 10500 $\text{cm}^{-1}$ (110)  660 nm, 15120 $\text{cm}^{-1}$ (sh) (680) 636 nm, 15700 $\text{cm}^{-1}$ (825) 602 nm, 16600 $\text{cm}^{-1}$ (sh) (520) --- 536 nm, 18650 $\text{cm}^{-1}$ (sh) (80)

L =	NCS <sup>-</sup> ( $\epsilon, (\text{mol/L})^{-1} \text{cm}^{-1}$ )	NCO <sup>-</sup> ( $\epsilon, (\text{mol/L})^{-1} \text{cm}^{-1}$ )	N <sub>3</sub> <sup>-</sup> ( $\epsilon, (\text{mol/L})^{-1} \text{cm}^{-1}$ )	Cl <sup>-</sup> ( $\epsilon, (\text{mol/L})^{-1} \text{cm}^{-1}$ )
Tp <sup>-</sup> =				
Tp <sup>t-Bu, Tn</sup>	1500 nm, 6670 cm <sup>-1</sup> (160) 930 nm, 10750 cm <sup>-1</sup> (380) 664 nm, 15060 cm <sup>-1</sup> (sh) (1880) 646 nm, 15480 cm <sup>-1</sup> (2390) 628 nm, 15920 cm <sup>-1</sup> (sh) (2110) 597 nm, 16750 cm <sup>-1</sup> (sh) (1270) 540 nm, 18520 cm <sup>-1</sup> (sh) (140)	not investigated	not investigated	1650 nm, 6060 cm <sup>-1</sup> (100) 942 nm, 10620 cm <sup>-1</sup> (90) --- 665 nm, 15040 cm <sup>-1</sup> (660) 640 nm, 15620 cm <sup>-1</sup> (700) 600 nm, 16670 cm <sup>-1</sup> (sh) (430) 550 nm, 18180 cm <sup>-1</sup> (sh) (60)

**Table S4.** Ligand-field parameters using the AOM derived for  $\text{Tp}^{\text{t-Bu,R}'}\text{CoL}$  complexes (values in  $\text{cm}^{-1}$ ).

L=	$\text{NCS}^-$	$\text{NCO}^-$	$\text{N}_3^-$	$\text{Cl}^-$
$\text{Tp}^- =$ $\text{Tp}^{\text{t-Bu,H}}[\text{L}_1]^a$				
$\epsilon_\sigma(\text{N-pz})$	3750 [3700]	3840	3840	3720
$\epsilon_\sigma(\text{L}), \epsilon_\pi(\text{L})$	2520 [2670], 0	2585, 0	2670, 0	2290, 440
$B$	690 [736]	703	680	712
$C$	2970 [3400]	3020	2920	3060
$\zeta$	420 [383]	(530) <sup>d</sup>	(530) <sup>d</sup>	(530) <sup>e</sup>
$\text{Tp}^{\text{t-Bu,Me}}$				
$\epsilon_\sigma(\text{N-pz})$	3790	3850	3850	3700
$\epsilon_\sigma(\text{L}), \epsilon_\pi(\text{L})$	3050, 0	2530, 0	2590, 0	2270, 275
$B$	664	715	678	713
$C$	2855	3070	2915	3065
$\zeta$	(455) <sup>b</sup>	(530) <sup>d</sup>	(530) <sup>d</sup>	(530) <sup>e</sup>
$\text{Tp}^{\text{t-Bu,Tn}}$				
$\epsilon_\sigma(\text{N-pz})$	3840	no experimental data	no experimental data	3760
$\epsilon_\sigma(\text{L}), \epsilon_\pi(\text{L})$	2585, 0			2290, 500
$B$	703			711
$C$	3020			3040
$\zeta$	(525) <sup>c</sup>			(530) <sup>e</sup>

<sup>a</sup> Referred to as  $\text{L}_1$  by Larrabee et al.<sup>13</sup> The parameters given in brackets are taken from their work, which found a lower magnitude zfs than that found here. They used  $C = 4.6B$ , while we use  $C = 4.3B$ .<sup>14</sup> In all cases, all  $\epsilon_\pi(\text{L}) = 0$  for the N-donor, pseudohalogen complexes, however, for the chloro complexes, cylindrical  $\epsilon_\pi(\text{Cl}) > 0$  was included.

<sup>b</sup> For this complex, it was not possible to match the magnitude of the observed zfs (see Table S5), even with the free-ion value for  $\zeta$  ( $533 \text{ cm}^{-1}$ <sup>15</sup>). The value given is one that is physically reasonable with respect to other complexes and to matching the electronic transitions.

<sup>c</sup> For this complex, it was possible to match exactly the magnitude of the observed zfs (see Table S5) with only nearly the free-ion value for  $\zeta$ .

<sup>d</sup> For this complex, it was possible to approach the magnitude of the observed zfs (see Table S5) with only the free-ion value for  $\zeta$ .

<sup>e</sup> Successful fits were obtained with  $\epsilon_\pi(\text{Cl}) = 0$ , however, inclusion of  $\pi$ -donation led to values for  $\Delta$  slightly closer to experiment.

**Table S5.** Comparison of HFEPR and MCD results for zfs ( $\Delta$ , in  $\text{cm}^{-1}$ ) in similar  $\text{Tp}^{\text{R,R}'}\text{CoL}$  complexes.<sup>a</sup>

L =	$\text{NCS}^-$	$\text{NCO}^-$	$\text{N}_3^-$	$\text{Cl}^-$
$\text{Tp}^- =$ $\text{Tp}^{-\text{i-Bu,H}}(\text{L}_1)^{\text{b}}$				
MCD <sup>c</sup>	3.7	3.0	---	---
HFEPR experimental <sup>c</sup> calculated <sup>d</sup>	+4.81 +4.81	+11.97 +10.46	+15.88 +11.24	+21.77 +17.71
$\text{Tp}^{-\text{i-Bu,Me}}$				
MCD	---	---	---	---
HFEPR experimental <sup>c</sup> calculated <sup>d</sup>	+5.40 -3.38	+10.84 +9.80	+12.75 +7.19	+23.04 +14.62
$\text{Tp}^{-\text{i-Bu,Tn}}$				
MCD	---	---	---	---
HFEPR experimental <sup>c</sup> calculated <sup>d</sup>	+6.89 +6.86	~11 ---	---	+25.58 +22.31
$\text{Tp}^{3-\text{i-Pr,4-Br}}(\text{L}_2)^{\text{e}}$				
MCD <sup>c</sup>	3.7	---	---	4.8
HFEPR	---	---	---	---
$\text{Tp}^{3-\text{Ph}}(\text{L}_3)^{\text{f}}$				
MCD <sup>c</sup>	3.1	3.0	4.2	---
HFEPR	---	---	---	---

<sup>a</sup> MCD results are taken from Larrabee et al.;<sup>13</sup> HFEPR from this work.

<sup>b</sup> Referred to as  $\text{L}_1$  by Larrabee et al.<sup>13</sup>

<sup>c</sup> MCD directly measured the zfs,  $|\Delta| = |2D\{1 + 3(E/D)^2\}^{1/2}| \approx 2D$ ; HFEPR directly determines  $D$  and  $E$ , including the sign of  $D$  (the sign of  $E$  is given that of  $D$ , by

convention). The sign is therefore provided for the experimental value of  $\Delta$  from HFEPR, but not from MCD.

<sup>d</sup> Values of  $\Delta$  were calculated using the ligand-field parameters given below in Table S4. The sign is obtained from a calculation of  $\langle S_z^2 \rangle$  for each of the two spin doublets of the ground state spin quartet; a positive sign results from the lower having  $\langle S_z^2 \rangle \approx 0.5$  and the upper having  $\langle S_z^2 \rangle \approx 1.5$ , and a negative sign from the opposite situation.

<sup>e</sup> The ligand is hydro[(3-*iso*-propyl-4-bromo)trispirazol-1-yl]borate and is referred to as L<sub>2</sub> by Larrabee et al.<sup>13</sup>

<sup>f</sup> Referred to as L<sub>3</sub> by Larrabee et al.<sup>13</sup>

## References

1. Trofimenko, S., *Polyhedron* **2004**, *23*, 197-203.
2. Gorrell, I. B.; Parkin, G., *Inorg. Chem.* **1990**, *29*, 2452-2456.
3. Rheingold, A. L.; Liable-Sands, L. M.; Golan, J. A.; Trofimenko, S., *Eur. J. Inorg. Chem.* **2003**, 2767-2773.
4. Uehara, K.; Hikichi, S.; Akita, M., *J. Chem. Soc., Dalton Trans.* **2002**, 3529-3538.
5. Olson, M. D.; Rettig, S. J.; Storr, A.; Trotter, J.; Trofimenko, S., *Acta Cryst.* **1991**, *C47*, 1543-1544.
6. Ferrence, G. M.; Beitelman, A. D., *Acta Cryst.* **2007**, *E63*, m153-m155.
7. Trofimenko, S.; Calabrese, J. C.; Thompson, J. S., *Inorg. Chem.* **1987**, *26*, 1507-1514.
8. Trofimenko, S.; Calabrese, J. C.; Domaille, P. J.; Thompson, J. S., *Inorg. Chem.* **1989**, *28*, 1091-1101.
9. Łukasiewicz, M.; Ciunik, Z.; Wołowiec, S., *Polyhedron* **2000**, *19*, 2119-2125.
10. Łukasiewicz, M.; Ciunik, Z.; Ruman, T.; Skóra, M.; Wołowiec, S., *Polyhedron* **2001**, *20*, 237-244.
11. Rheingold, A. L.; Liable-Sands, L. M.; Yap, G. P. A.; Trofimenko, S., *Chem. Commun.* **1996**, 1233 - 1234.
12. Calabrese, J. C.; Trofimenko, S., *Inorg. Chem.* **1992**, *31*, 4810-4814.
13. Larrabee, J. A.; Alessi, C. M.; Asiedu, E. T.; Cook, J. O.; Hoerning, K. R.; Klingler, L. J.; Okin, G. S.; Santee, S. G.; Volkert, T. L., *J. Am. Chem. Soc.* **1997**, *119*, 4182-4196.
14. Figgis, B. N.; Hitchman, M. A., *Ligand Field Theory and its Applications*. Wiley-VCH: New York, 2000.
15. Bendix, J.; Brorson, M.; Schäffer, C. E., *Inorg. Chem.* **1993**, *32*, 2838-2849.

**Figure S1.** Molecular structure of  $\text{Tp}^{t\text{-Bu,H}}\text{Co}(\text{NCO})$  determined by x-ray crystallography in this work. Thermal ellipsoid plots are at the 50% probability level.

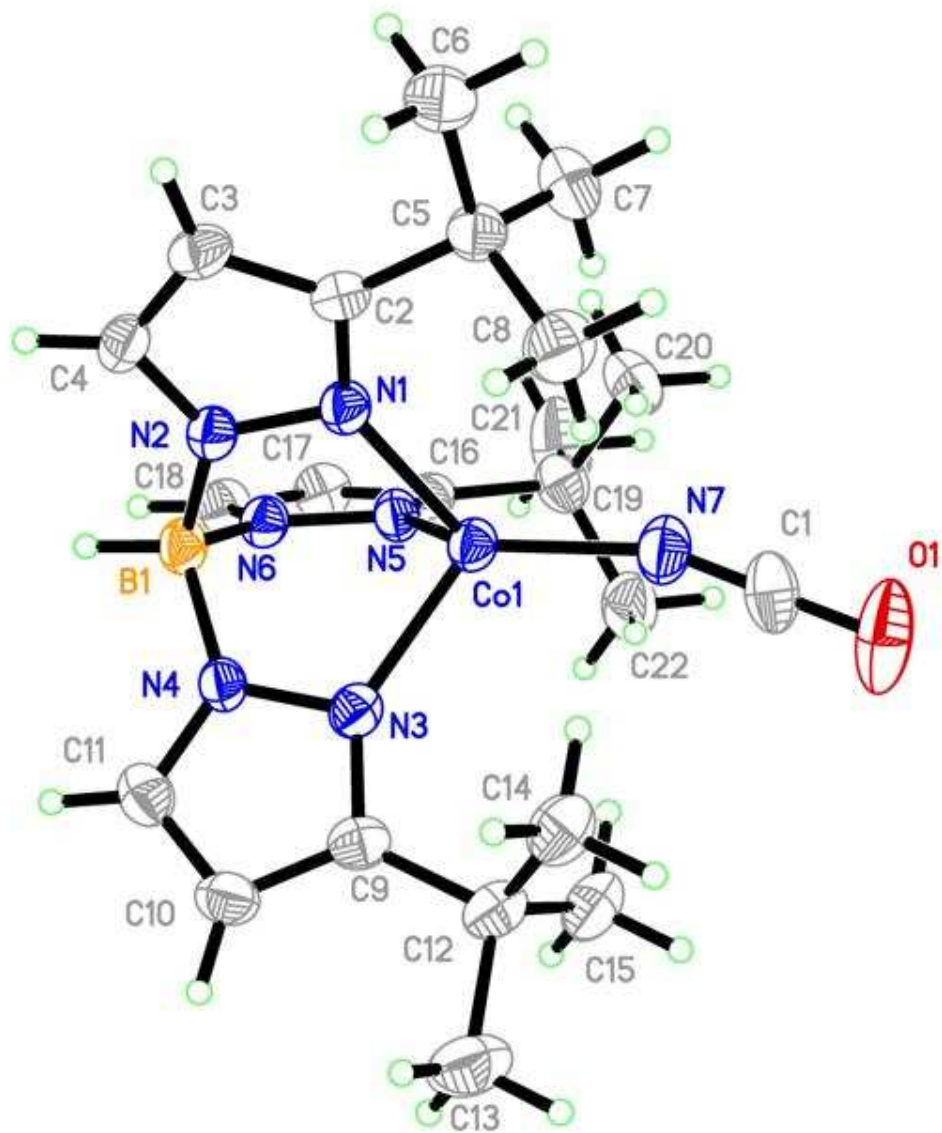


**Figure S2.** Molecular structure of  $\text{Tp}^{t\text{-Bu,H}}\text{CoN}_3$  determined by x-ray crystallography in this work. Thermal ellipsoid plots are at the 50% probability level.

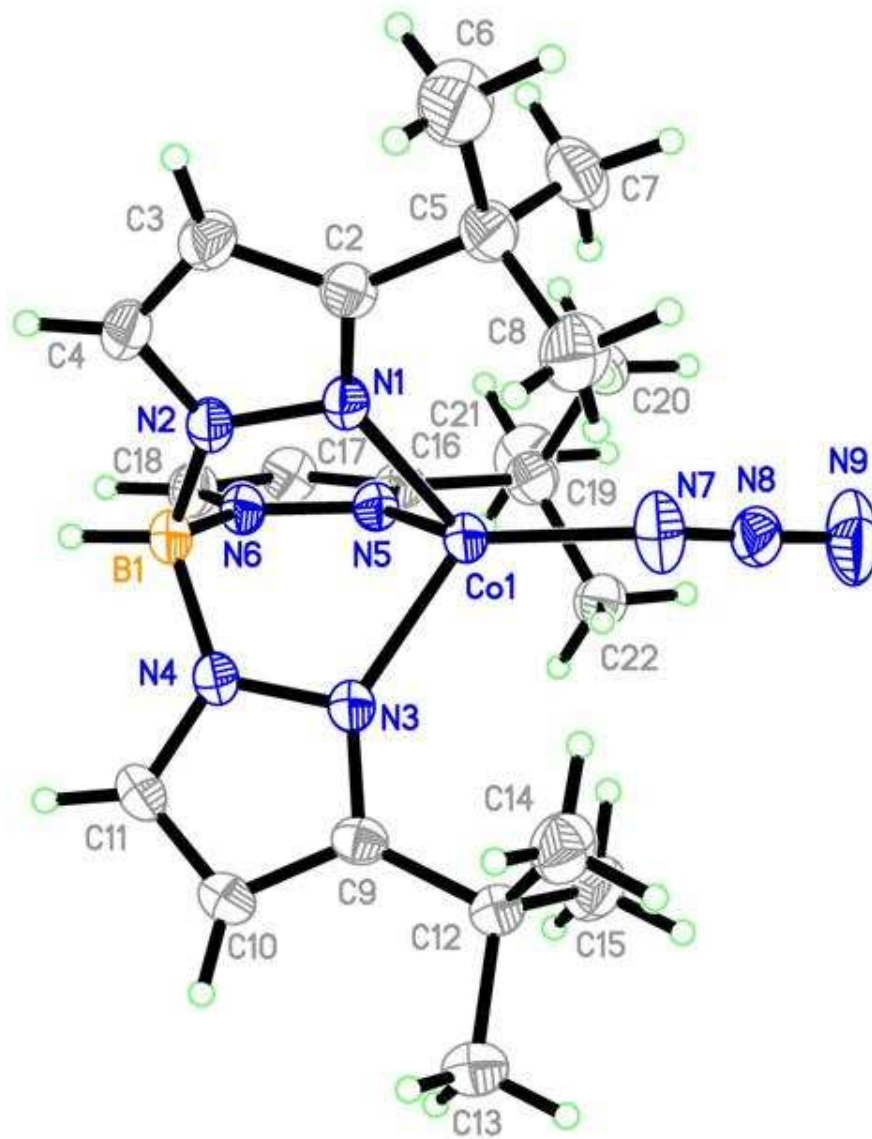


**Figure S3.** Molecular structure of  $\text{Tp}^{t\text{-Bu,Me}}\text{CoCl}$  determined by x-ray crystallography in this work. Thermal ellipsoid plots are at the 50% probability level. This structure is of an inversion twin (fraction = 0.442(0.015)).

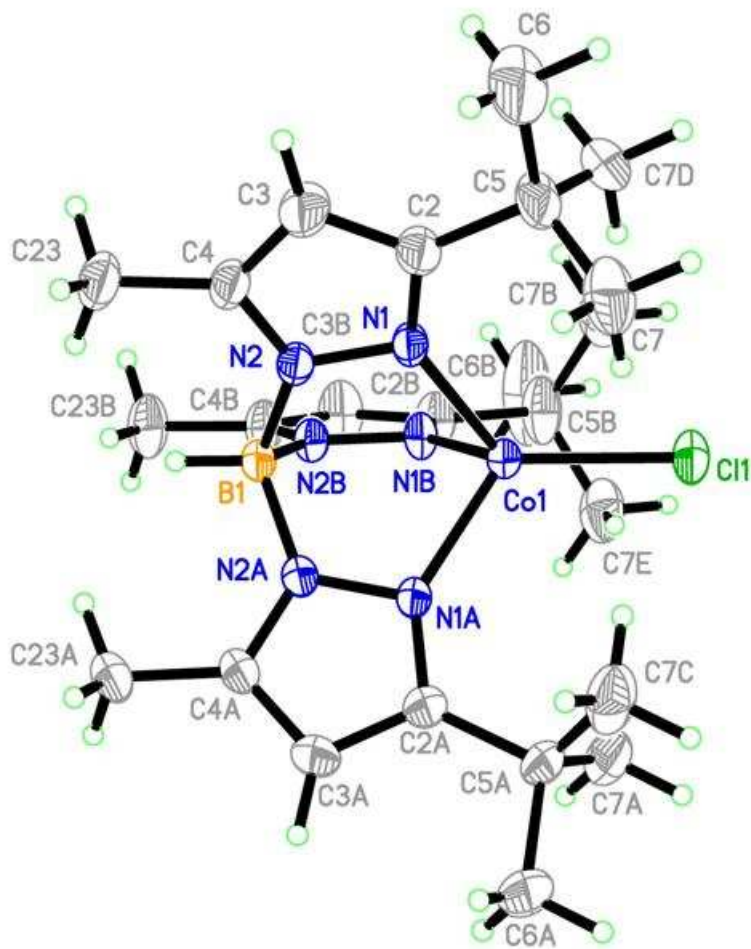


**Figure S4.** Molecular structure of  $\text{Tp}^{t\text{-Bu,Me}}\text{Co}(\text{NCS})$  determined by x-ray crystallography in this work. Thermal ellipsoid plots are at the 50% probability level.

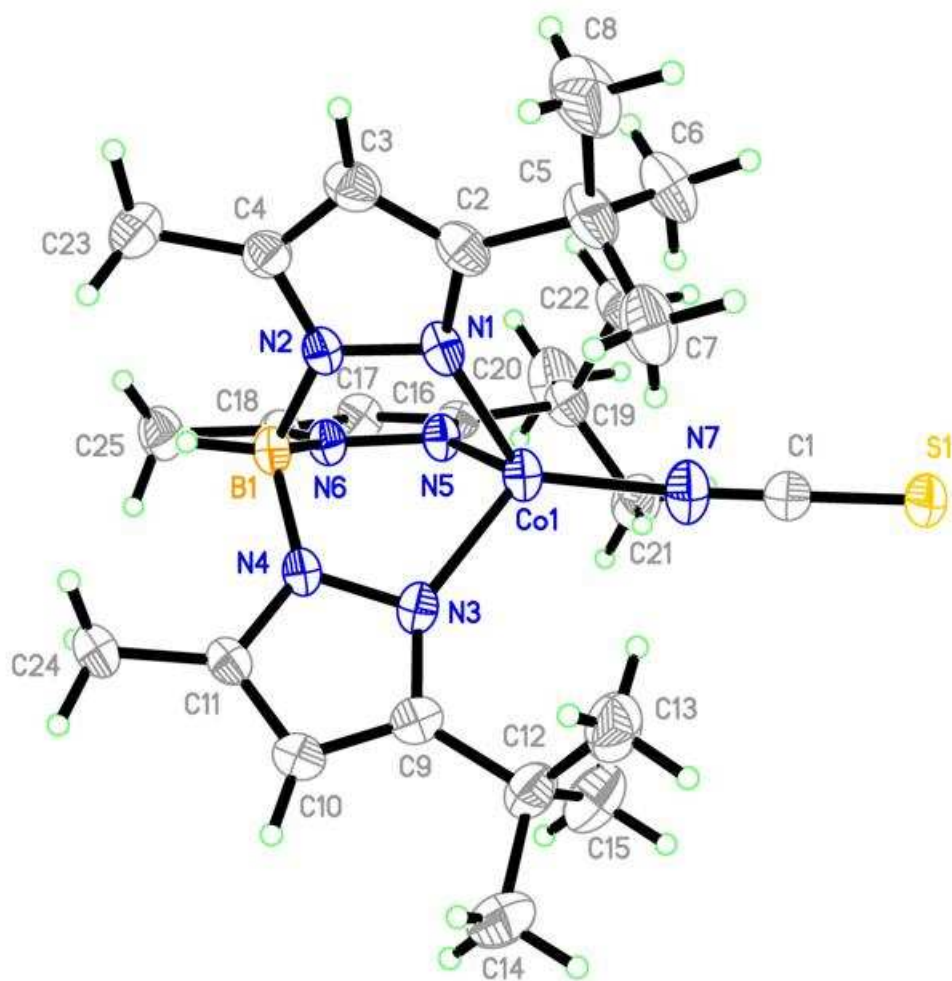


**Figure S5.** Molecular structure of  $\text{Tp}^{t\text{-Bu,Me}}\text{Co}(\text{NCO})$  determined by x-ray crystallography in this work. Thermal ellipsoid plots are at the 50% probability level. Disorder in one of the *t*-Bu groups (C13-C15) is shown; this disorder can lead to warnings in the CIF.

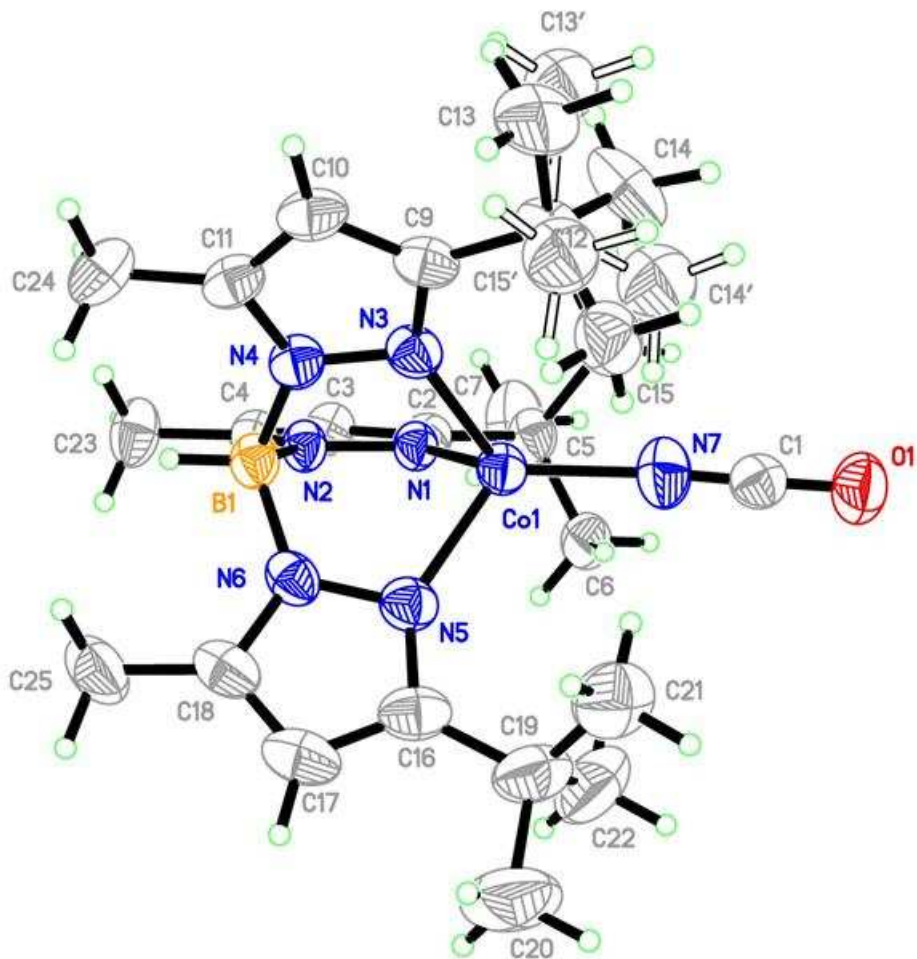


**Figure S6.** Molecular structure of  $\text{Tp}^{t\text{-Bu,Me}}\text{CoN}_3$  determined by x-ray crystallography in this work. Thermal ellipsoid plots are at the 50% probability level. Disorder in the azido ligand is shown. A disordered molecule of crystallization of toluene from solvent is also shown; these disorders can lead to warnings in the CIF.

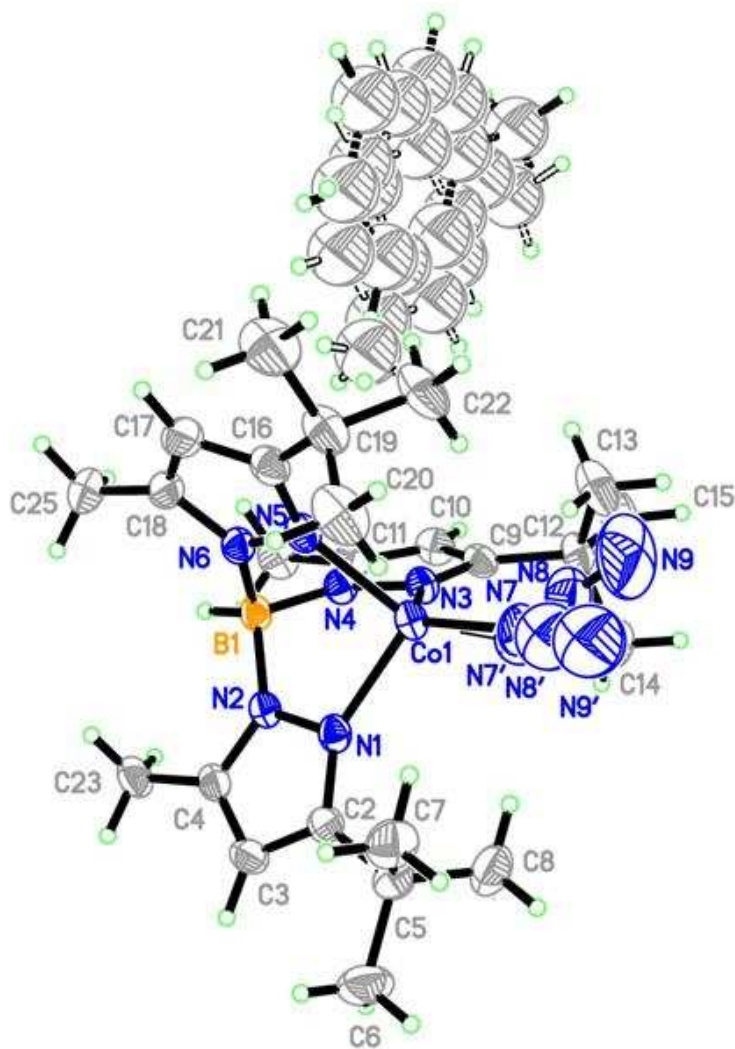


**Figure S7.** Molecular structure of  $\text{Tp}^{t\text{-Bu,Tn}}\text{CoCl}$  determined by x-ray crystallography in this work. Thermal ellipsoid plots are at the 50% probability level. Disorder in one of the thienyl substituents is indicated. Disordered molecules of crystallization of dichloromethane from solvent also shown; these disorders can lead to warnings in the CIF.

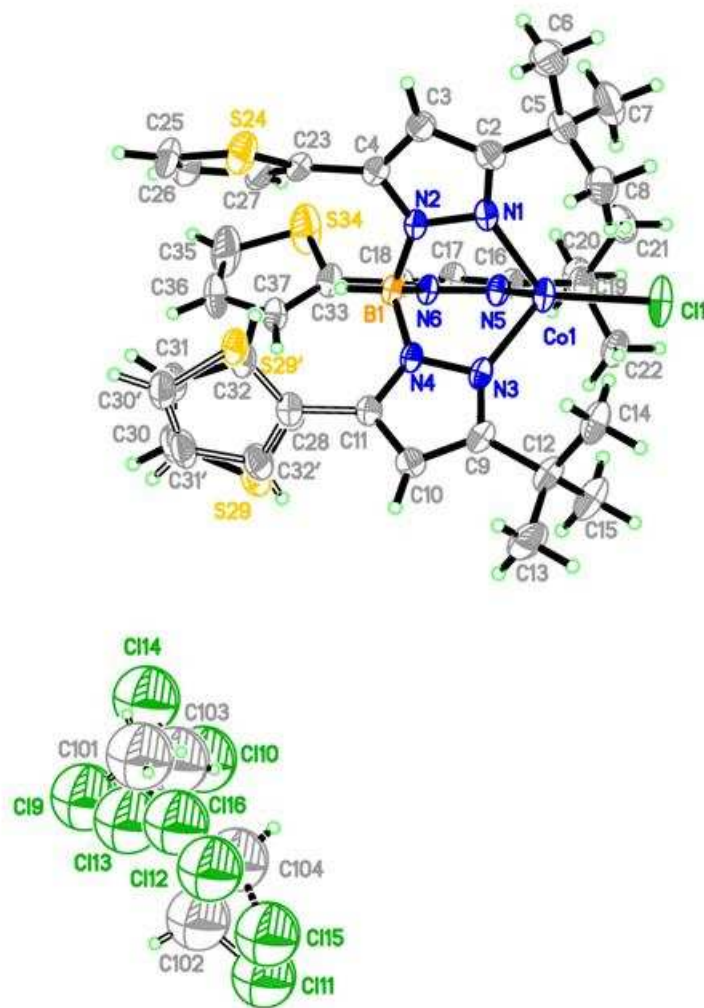


**Figure S8.** Molecular structure of  $\text{Tp}^{t\text{-Bu,Tn}}\text{Co}(\text{NCS})$  determined by x-ray crystallography in this work. Thermal ellipsoid plots are at the 50% probability level. Disorder in two of the thienyl substituents and in the thiocyanato ligand is indicated; these disorders can lead to warnings in the CIF.

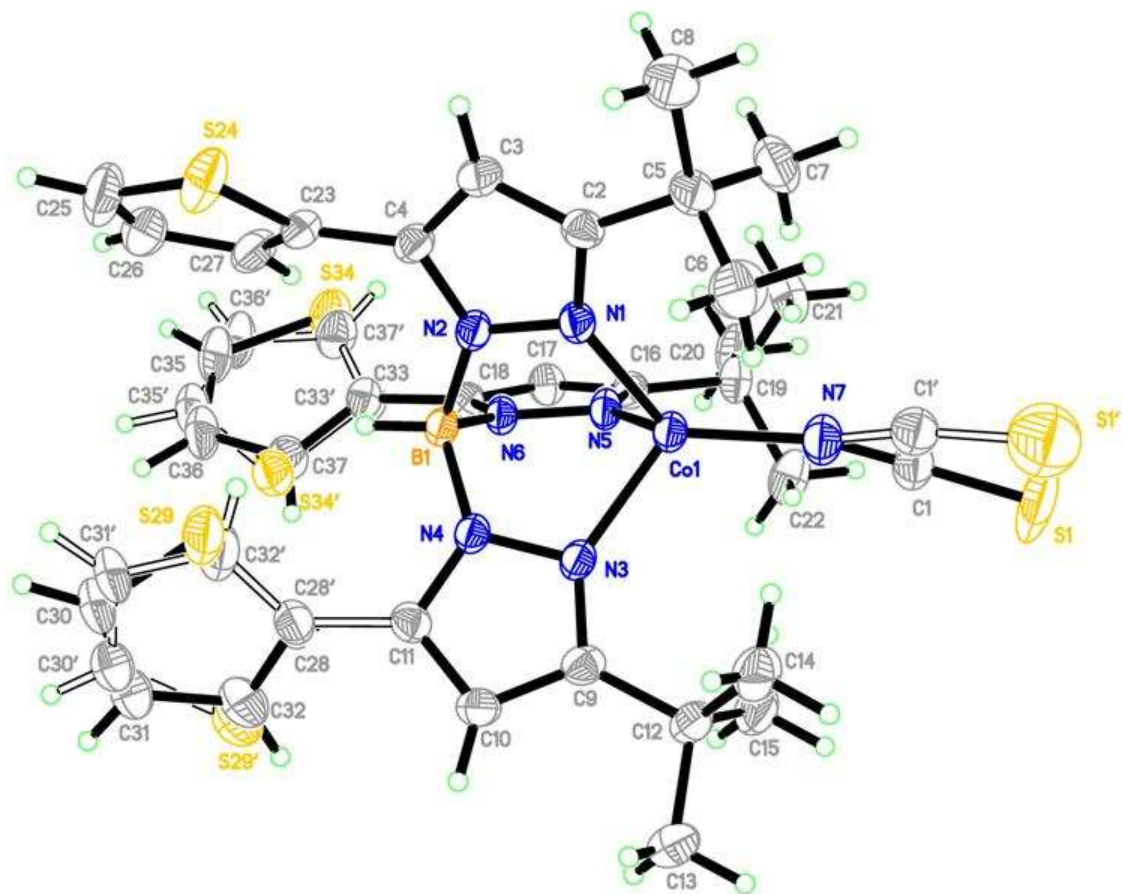


**Figure S9.** Electronic absorption spectra for  $\text{Tp}^{\text{R,R}'}\text{CoL}$  ( $\text{R} = t\text{-Bu}$ ,  $\text{R}' = \text{H, Me, Tn}$ ;  $\text{L} = \text{NCS}^-$ ,  $\text{NCO}^-$ ,  $\text{N}_3^-$ ,  $\text{Cl}^-$ ) complexes in  $\text{CCl}_4$  solution at room temperature, scaled to their molar absorptivity (in  $(\text{mol/L})^{-1}\text{cm}^{-1}$ ). The specific complexes are identified by color of trace, as indicated on the figure; the corresponding labels are in approximate order of maximum absorptivity from highest (top label) to lowest (bottom label).

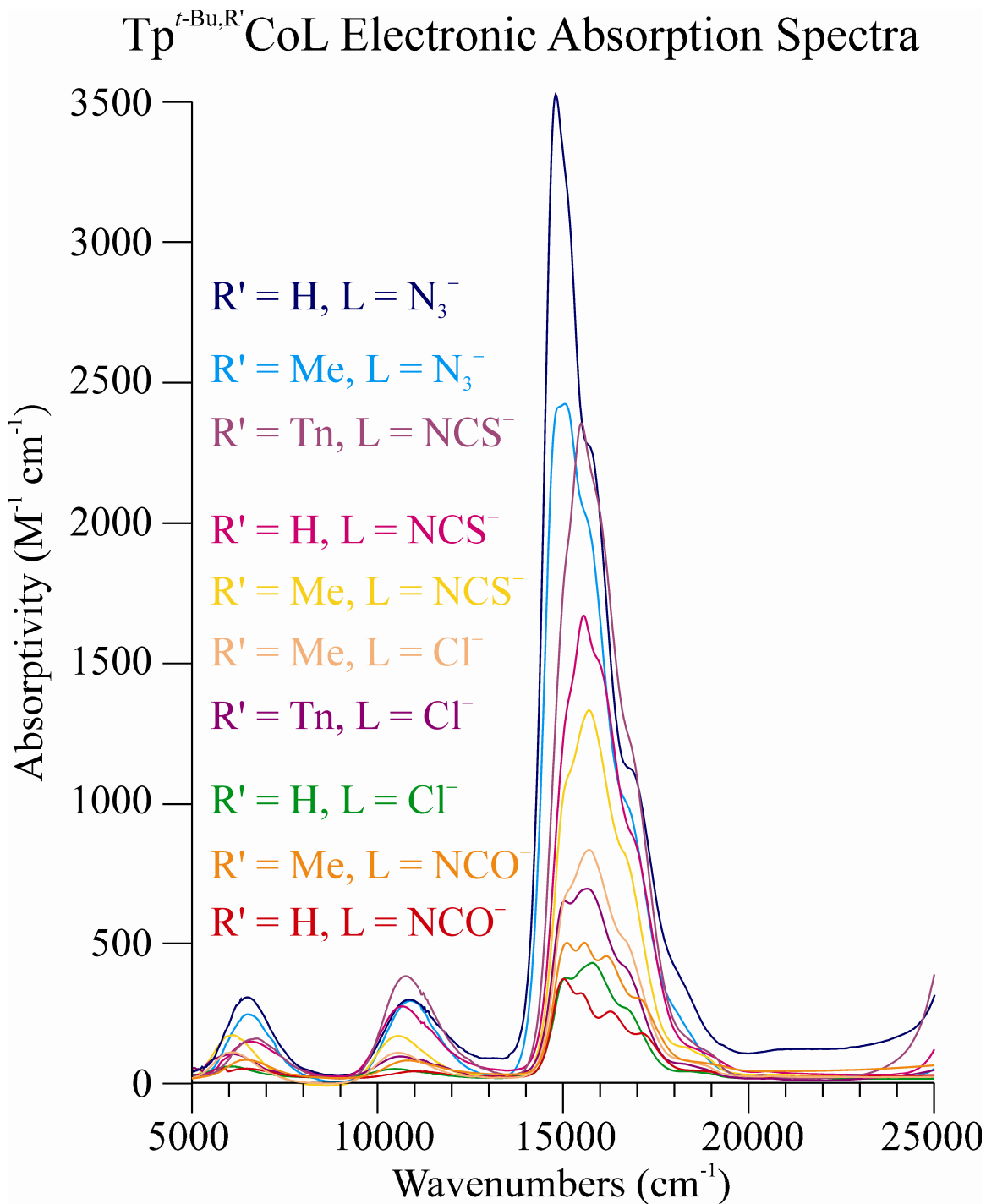


**Figure S10.** 2-D field/frequency (or quantum energy) maps of EPR turning points for the  $\text{Tp}^{t\text{-Bu,Me}}\text{CoL}$  series: (a)  $L = \text{NCS}^-$ ; (b)  $L = \text{NCO}^-$ ; (c)  $L = \text{N}_3^-$ ; (d)  $L = \text{Cl}^-$ . The squares are experimental points, and the curves were simulated using best-fit spin Hamiltonian parameters as in Table 3. Red curves denote turning points with  $B_0 \parallel x$ , blue curves with  $B_0 \parallel y$ , black curves with  $B_0 \parallel z$ , while the green curve in plot (a) is an off-axis turning point branch. The data set corresponds to  $T = 4.5$  K

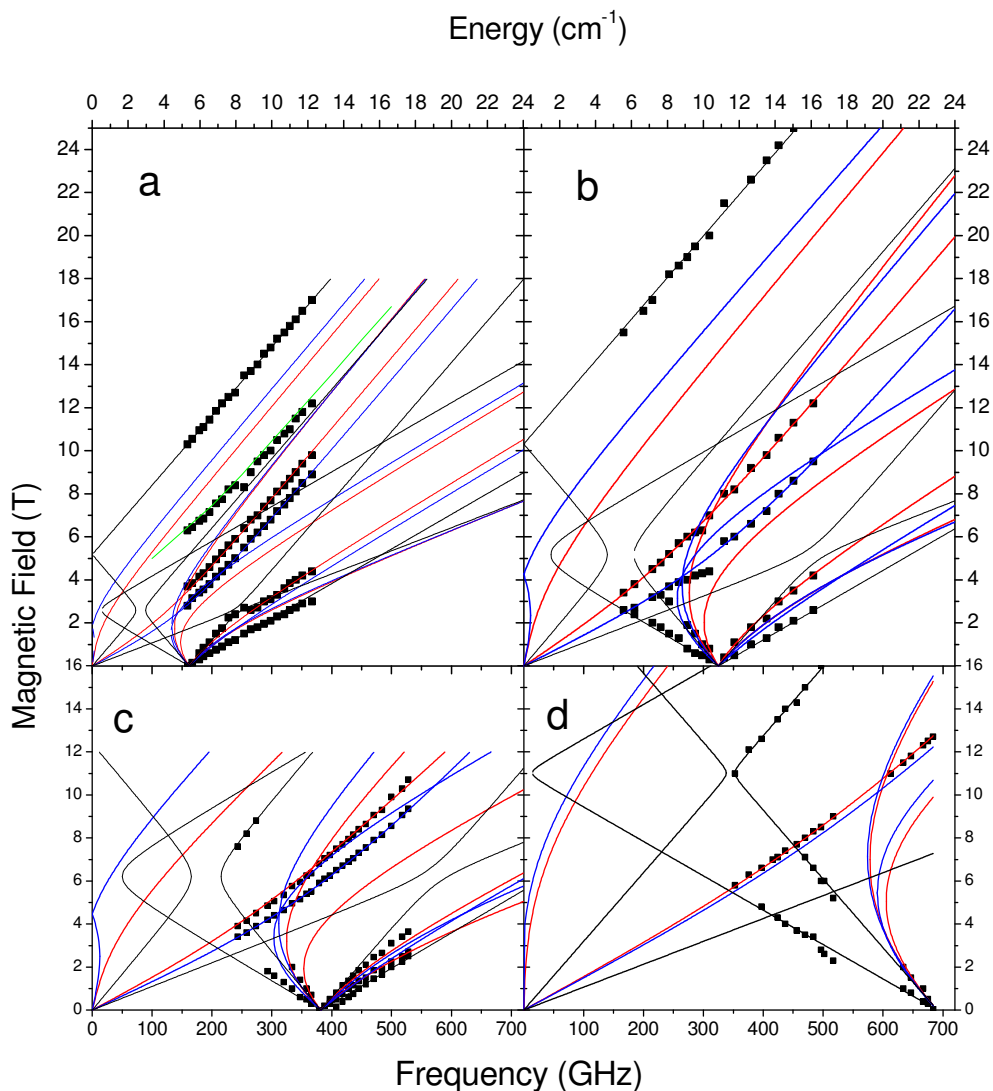


**Figure S11.** 2-D field/frequency (or quantum energy) maps of EPR turning points for the  $\text{Tp}^{\text{-Bu,Me}}\text{CoL}$  series: (a)  $\text{L} = \text{NCS}^-$ ; (b)  $\text{L} = \text{Cl}^-$ . The squares are experimental points, and the curves were simulated using best-fit spin Hamiltonian parameters as in Table 3. Red curves denote turning points with  $B_0 \parallel x$ , blue curves with  $B_0 \parallel y$ ; black curves with  $B_0 \parallel z$ , while the green curve in plot (a) is an off-axis turning point branch. The data set corresponds to  $T = 4.5$  K.

